

Serveur Académique Lausannois SERVAL serval.unil.ch

Author Manuscript

Faculty of Biology and Medicine Publication

This paper has been peer-reviewed but does not include the final publisher proof-corrections or journal pagination.

Published in final edited form as:

Title: Single cell analysis reveals similar functional competence of dominant and nondominant CD8 T-cell clonotypes.

Authors: Speiser DE, Wieckowski S, Gupta B, Iancu EM, Baumgaertner P, Baitsch L, Michielin O, Romero P, Rufer N

Journal: Proceedings of the National Academy of Sciences of the United States of America

Year: 2011 Sep 13

Volume: 108

Issue: 37

Pages: 15318-23

DOI: 10.1073/pnas.1105419108

In the absence of a copyright statement, users should assume that standard copyright protection applies, unless the article contains an explicit statement to the contrary. In case of doubt, contact the journal publisher to verify the copyright status of an article.

**Single cell analysis reveals similar functional competence of dominant
and non-dominant CD8 T-cell clonotypes**

Daniel E. Speiser^{1,*}, Sébastien Wieckowski^{2,*}, Bhawna Gupta², Emanuela M. Iancu²,
Petra Baumgaertner¹, Lukas Baitsch¹, Olivier Michielin^{1,3}, Pedro Romero¹, and
Nathalie Rufer^{1,2,3}

¹Ludwig Center for Cancer Research of the University of Lausanne, Lausanne,
Switzerland

²Department of Research, University Hospital Center and University of Lausanne,
Lausanne, Switzerland

³Multidisciplinary Oncology Center (CePO), University Hospital Center, Lausanne,
Switzerland

* These authors contributed equally to this work

Address correspondence to: Nathalie Rufer, PhD, Department of Research,
CHUV/University of Lausanne, c/o HO, niv 5, Avenue Pierre-Decker 4, CH-1011
Lausanne, Switzerland; Nathalie.Rufer@unil.ch and Daniel E. Speiser, Ludwig
Center for Cancer Research of the University of Lausanne, c/o HO, niv 5, Avenue
Pierre-Decker 4, CH-1011 Lausanne, Switzerland; Daniel.Speiser@hospvd.ch.

Running title: Impact of peptide vaccination on CD8 T-cell responses

Keywords: human, melanoma, vaccination, EBV, CMV, CD8 T-cells, single cell, TCR repertoire, clonotype, differentiation, gene/protein expression, cytolysis

Abbreviations: IFA, Incomplete Freund's Adjuvant; EBV, Epstein-Barr virus; CMV, Cytomegalovirus

Author contributions: D.E.S., S.W. and N.R. designed research. D.E.S. and O.M. were clinical investigators. S.W., B.G., E.M.I., P.B., L.B., P.R. and N.R. performed research and analyzed data. D.E.S., S.W. and N.R. wrote the manuscript.

ABSTRACT

Immune protection from infectious diseases and cancer is mediated by individual T-cells of different clonal origin. Their functions are tightly regulated but not yet fully characterized. Understanding the contribution of each T-cell will improve the prediction of immune protection based on laboratory assessment of T-cell responses. Here we developed novel techniques for simultaneous molecular and functional assessment of single CD8 T-cells directly *ex vivo*. We studied two groups of melanoma patients, after vaccination with two closely related tumor antigenic peptides. Vaccination induced T-cells with strong memory and effector functions, as found in virtually all T-cells of the first patient group, and fractions of T-cells in the second group. Interestingly, high functionality was not restricted to dominant clonotypes. Rather, dominant and non-dominant clonotypes acquired equal functional competence. In parallel, this was also found for EBV- and CMV-specific T-cells. Thus, the non-dominant clonotypes may contribute similarly to immunity as their dominant counterparts.

¥body

INTRODUCTION

Naturally acquired self-antigen (tumor)-specific T-cell responses can be detected in most cancer patients with advanced disease, however, they often fail to control or eliminate the disease, in contrast to many virus-specific CD8 T-cell responses (1, 2). This likely reflects the impact of both central and peripheral tolerance in shaping self antigen-specific T-cell repertoires. Vaccination against cancer aims to generate and/or boost effective type 1 immune responses (Th1 and CD8 T-cell activation) to destroy tumor cells and prevent tumor progression. These goals are similar to those set for vaccines designed to treat chronic viral diseases. There is a great need to characterize and determine the biological similarities and differences between protective (e.g. EBV- and CMV-specific) and non-protective (e.g. tumor-specific) T-cell responses.

Only limited data is available regarding T-cell clonotype dynamics in therapeutic vaccine settings. Yet, clonotypic analyses provide great insight, mostly because T-cell clonotypes can be followed in a straightforward manner at any time and body location using the TCR as a clonotypic marker (3). For example, combined *ex vivo* analysis of T-cell differentiation and clonality allowed the identification of a naturally primed T-cell clone in a melanoma patient (4). The progeny of this clone dominated the CD8 T-cell response to the tumor antigen Melan-A^{MART-1}, similarly to the clonal expansions observed in virus-specific T-cell responses (5-7). However, in several patients and healthy individuals, one can also find large numbers of low/non-dominant T-cell clonotypes among tumor-specific (8) and virus-specific (6) CD8 T-cells. Remarkably, not only the dominant, but also the subdominant virus-specific clonotypes were maintained stably over years, keeping the TCR repertoire composition constant (6). These observations raise the question whether dominant T-

cell clonotypes alone are sufficient, or whether low/non-dominant clonotypes are also functionally competent and may contribute to immune protection.

Historically, research has mostly focused on dominant T-cell clonotypes, whereas the *in vivo* functions of non-dominant clonotypes remain poorly characterized, likely because of technical limitations. Therefore, we developed new methods suitable for the *ex vivo* functional assessment of individual T-cells, combined with clonotypic characterization. With this strategy, we analyzed clonal responses of tumor antigen-specific T-cells from melanoma patients, in parallel to protective EBV- and CMV-specific T-cells. The melanoma patients had received potent low dose synthetic vaccines composed of Melan-A₂₆₋₃₅ peptide, CpG-ODN 7909 and Incomplete Freund's Adjuvant (IFA). This vaccine consistently induced strong T-cell responses that were easily detectable by direct *ex vivo* analysis (9), not only when the Melan-A A27L analog peptide (optimized for enhanced HLA-A*0201 binding) was used for vaccination, but also with the weakly antigenic native peptide (10). We have previously shown that the native peptide induced T-cell responses with increased capacity to recognize tumor cells and increased overall T-cell functionality (10). Here, we demonstrate that this superior tumor reactivity was associated with enhanced effector cell activation of nearly all individual T-cells. Importantly, these properties were found in both dominant and non-dominant tumor antigen-specific T-cell clonotypes. Our data reveal that T-cell functions are determined primarily by the antigen used for vaccination and the stage of T-cell differentiation, but are similar in dominant and non-dominant clonotypes participating in a CD8 T-cell response.

RESULTS

Strong expansion and differentiation of tumor antigen-specific CD8 T-cells following peptide vaccination. Fifteen HLA-A2+ patients with advanced metastatic melanoma received monthly vaccinations consisting of either the native Melan-A unmodified peptide (EAAGIGILTV, i.e. “EAA”) or the analog Melan-A A27L modified heteroclitic peptide (ELAGIGILTV, i.e. “ELA”), combined with CpG-ODN 7909 and emulsified in IFA (Table S1). Using fluorescent HLA-A2/peptide multimers for *ex vivo* analysis, high frequencies of Melan-A specific CD8 T lymphocytes were detected in all patients, and strongly increased as compared to before vaccination (defined as time 0; Fig. 1A). We found progressive accumulation of late-differentiated effector-memory EM28- Melan-A-specific T-cells (defined thereafter as “effector-like” cells), which appeared early in some patients and later in others, independent of whether patients received native or analog peptide. The established T-cells were maintained over extended periods of time while patients continuously received monthly booster vaccinations.

Vaccination-induced T-cell responses are composed of dominant and non-dominant clonotypes. We characterized in depth the *ex vivo* TCR repertoire diversity resulting from clonal selection of tumor-reactive T-cells in patients vaccinated either with the native (EAA; n = 5) or the analog (ELA; n = 10) Melan-A peptide (Fig. 1A), as described previously (4). Primed effector-memory EM28+ cells (also defined as early-differentiated cells) displayed large polyclonal TCR repertoires with a diverse usage of the 22 different BV families studied, and high variability in CDR3 size. However, 12 of the 15 patients showed progressive restrictions in TCR

BV/CDR3 diversity from EM28⁺ to EM28⁻ T-cell subsets (Fig. 1B), which was accompanied by preferential expansion of several tumor antigen-specific co-dominant clonotypes of intermediate (low) to high frequencies (Fig. 1C), irrespective of whether native or analog peptide was used for vaccination. These clonotypes made up in average around 55% of the late-differentiated EM28⁻ “effector-like” subset, but only 25% of the early-differentiated EM28⁺ “effector-memory” T-cells. Our data revealed the establishment of relatively few (between 7 to 15) co-dominant tumor-specific T-cell clonotypes that were highly specific for each patient as defined by their private TCR BV CDR3 β signatures (Fig. S1A). Importantly, both subsets also contained non-dominant T-cell clonotypes, but these were more frequent in EM28⁺ than in EM28⁻ T-cells.

Altogether, these findings show that similarly to protective virus-specific responses (6), vaccination-induced tumor-specific T-cell responses are composed of dominant and non-dominant clonotypes (Fig. 1C). Moreover, clonotype selection and expansion of tumor antigen-specific T-cells along cell differentiation resembled closely those observed in anti-EBV responses (6). These data were obtained following cell sorting with multimers bearing the analog peptide. Similar results were obtained with multimers bearing the native peptide (Fig. S1B), thus indicating that the two multimers efficiently bound to all Melan-A-specific T-cells with similar fine specificity to analog or native peptide, in line with our previous report (10).

Enhanced expression of multiple effector mediators by native peptide vaccination-induced T-cells, closely resembling highly differentiated CMV-specific T-cells. To qualitatively assess the effect of native versus analog peptide vaccination, we developed techniques for combined *ex vivo* analysis of molecular and

functional properties at the single-cell level, using a modified RT-PCR protocol, enabling the detection of specific cDNAs after global amplification of expressed mRNAs from individual sorted T-cells (Fig. 2 and Fig. S2A). We found that most early-differentiated EM28⁺ T-cells issued from patients vaccinated with the analog/ELA peptide contained low detectable levels of mRNA coding for effector mediators such as IFN- γ , perforin, granzyme B and C-type killer cell lectin-like receptor CD94, while expressing measurable levels of mRNA coding for the costimulatory molecule CD27 and the cytokine receptor IL-7R α (CD127). Increased expression of effector mediators was observed in late-differentiated EM28⁻ T-cells after analog peptide vaccination, and was concomitant with down-regulation of costimulatory and cytokine receptors (Fig. 2A and 2B). EBV-specific T-cells also presented distinct mRNA expression patterns along cellular differentiation, but globally these cells remained less differentiated than tumor- or CMV-specific T-cells, in agreement with our recent report (6). A remarkable finding was that tumor antigen-specific T-cells generated following native/EAA peptide vaccination exhibited similar detectable levels of effector mediators than those observed in CMV-specific T-cells. Remarkably, such expression patterns were already found within the EM28⁺ compartment, despite the co-expression of early-differentiated CD27 and IL-7R α gene transcripts (Fig. 2A and 2B). These cells also showed more poly-functional expression profiles compared with the corresponding EM28⁺ T-cells specific for ELA and EBV epitopes (Fig. S2B).

A hierarchical clustering performed on a total of 529 single-cell samples identified 5 distinct clusters based on the differential co-expression patterns of the 6 studied genes (Fig. 2C). The Heat-map analysis further allowed determining the repartition of these clusters within the single-cell samples of each T-cell subset. Strikingly, it revealed

that the early-differentiated EM28⁺ T-cells induced by the native/EAA peptide were comprised within the second group formed by the late-differentiated EM28⁻/EMRA “effector-like” ELA⁻, EAA⁻, and CMV-specific T-cells.

The mRNA content correlated with protein expression of CD27, IL-7R α , IFN- γ , perforin and granzyme B, as confirmed by extended *ex vivo* multi-parameter flow cytometry analyses of T-cells from fifteen vaccinated melanoma patients as well as seven healthy individuals with persistent herpes virus infections (Fig. 3; Fig. S3). Of note, we observed differences in mRNA and protein expression by specific T-cells from the same subset that may reflect biological variations among different individuals. The expression of CD57, a marker of cellular differentiation, perforin and granzyme B were found to be up-regulated even in the early-differentiated EM28⁺ T-cell subset in patients after native peptide vaccination (Fig. 3). Production of IFN- γ and up-regulation of LAMP-1 (CD107a) by tumor-specific T-cells showed a tendency to increased effector properties after vaccination with native peptide (Fig. S3). Altogether, our results indicate that vaccination with the native but not analog tumor antigen resulted in enhanced activation and poly-functionality *in vivo* of virtually all specific CD8 T-cells, independently of CD28, CD27 and IL-7R α co-expression, and resembling highly differentiated CMV-specific responses.

Both T-cell differentiation and the peptide used for vaccination determine the functional profile of individual T-cell clonotypes. The powerful single-cell based approach allowed for the first time to analyze *in vivo* gene expression of (multiple representatives of) individual T-cell clonotypes. By this strategy, we compared clonotype performance after vaccination with analog versus native peptide based on

their frequencies. The functional profiles of dominant T-cell clonotypes (Fig. 4A) largely overlapped with those of the corresponding early- or late-differentiated subset, respectively (Fig. S2B). For instance, the dominant EM28⁺ clonotypes from patient LAU 618/ELA were less poly-functional and shared the gene expression profile found in early-differentiated EM28⁺ subsets from analog peptide vaccinated patients. Conversely, the profiles of the dominant native peptide vaccination-induced clonotypes from patient LAU 1013 were highly poly-functional, and corresponded to the overall gene expression profiles found within respective EM28⁺ and EM28⁻ subsets. Gene expression signatures of non-dominant tumor-specific T-cells (Fig. 4B) also correlated tightly with the subset of origin (e.g. EM28⁺ or EM28⁻) and the type of peptide used for vaccination (e.g. native or analog peptide). Similar observations were made for the dominant and non-dominant clonotypes found in EBV- and CMV-specific immune responses. In summary, the functional profiles of dominant and non-dominant T-cell clonotypes were primarily determined by antigen and differentiation stage, and not by their degree of prevalence.

Efficient target cell killing by T-cells of both dominant and non-dominant clonotypes from patients vaccinated with native peptide. We assessed the ability of native and analog peptide vaccination-induced tumor-specific T-cells to recognize and kill tumor cells (Fig. 5). As expected, most T-cell clones derived from the late-differentiated “effector-like” EM28⁻ subset were able to kill the Melan-A-expressing tumor cell line Me290, irrespectively of the peptide used for vaccination. However, T-cell clones derived from the early-differentiated EM28⁺ subset following analog peptide vaccination were often deficient in cytotoxic function. In contrast, a large majority of T-cell clones derived from the same EM28⁺ subset from patients

vaccinated with the native peptide efficiently killed the Me290 cell line. Strikingly, this occurred regardless of their clonal prevalence (e.g. dominant or non-dominant frequencies; Fig. 5B). The results obtained by such analyses using *in vitro* generated clones are in full agreement with the *ex vivo* gene (Fig. 2) and protein (Fig. 3) expression patterns, thus allowing us to draw conclusions with respect to the *in vivo* status of T-cells. Furthermore, we have previously demonstrated that these T-cell clones maintained their specific killing properties despite several weeks of *in vitro* culture (11). Indeed, high and low cytotoxic activity correlated well with high and low *in vitro* and *in vivo* expression of granzyme B and perforin, respectively (11).

Collectively, these data show differential cytotoxicity of analog peptide-generated T-cell clones depending on the *in vivo* differentiation stage. In contrast to analog peptide vaccination, strong cytolytic activity was observed after vaccination with the native peptide, regardless of the type of subset (i.e. clones isolated from EM28+ or EM28-). Similar efficient target cell killing was observed between dominant and non-dominant T-cell clonotypes in cytotoxic assays against HLA-A2^{pos} T2 cells pulsed with graded peptide concentration (Fig. S4). Our findings reveal a surprising functional competence not only of the frequent clonotypes, but also of the rare clonotypes among epitope-specific T-cell populations.

DISCUSSION

T-cells from peptide vaccinated melanoma patients provide an ideal opportunity to assess possible effects of small antigenic differences in defined therapeutic vaccines on memory and effector cell functions, stage of differentiation, and clonotype selection. Here, we demonstrate that vaccination with native peptide induced functional T-cells in nearly all dominant and low/non-dominant clonotypes. In contrast, many T-cells remained poorly functional after vaccination with analog peptide, despite similar clonotype-dependent differentiation. The present study shows that single-cell analysis provides reliable quantification of individual cells expressing particular genes, as confirmed by protein expression analyses. Moreover, our strategy was highly sensitive to identify tumor-reactive T-cell clonotypes and to assess their frequencies. Finally, our results from these direct *ex vivo* analyses were in excellent agreement with the data obtained with large numbers of T-cell clones generated *in vitro* (6). An analogous approach has been previously and successfully applied to study cell heterogeneity during *in vivo* CD8 T-cell differentiation (12, 13). Recently, single cell gene expression profiling was shown to allow identifying qualitative differences in CD8 T-cell responses elicited by different gene-based vaccines (14).

We found that anti-tumor T-cell function was primarily determined by the type of peptide used for vaccination (native versus analog) and was not inherent to the degree of prevalence of a given T-cell clonotype (dominant versus non-dominant). Moreover, similar distributions in memory/effector gene expression signatures were found between T-cell clonotypes issued from the same subset of differentiation. Comparable observations were made for EBV- and CMV-specific T-cells, indicating that the functional profile of individual T-cells is also influenced by the differentiation status. As a consequence, most if not all clonotypes from a given

subset of differentiation and participating in a tumor (self) or viral (non-self) T-cell response may be equally competent. Selection of a T-cell repertoire composed of low/non-dominant and dominant clonotypes could serve to promote clonotypic diversity, while maintaining functional competence. These results are consistent with the report by Messaoudi and colleagues (15) that a diverse TCR repertoire but not a restricted one can mobilize protective antigen-specific T-cells of high avidity and efficient target cell killing.

Our data also show that a synthetic vaccine (i.e. decapeptide, CpG-ODN and IFA (9)) was able to trigger a similar composition of T-cell clonotypes as in viral infections (5, 7), and particularly in EBV-specific T-cell responses (6). Responding T-cells were composed of clonotypes of varying frequencies (dominant, subdominant and non-dominant), yet their clonal prevalence was dependent on the differentiation stage. Late-differentiated EM28⁻ (“effector-like”) cells consisted primarily of patient-specific dominant (high frequency) and subdominant (low frequency) clonotypes with long-term persistence. In contrast, the early-differentiated EM28⁺ subset (that includes “effector-memory” cells) contained mostly non-dominant clonotypes with only a small fraction of co-dominant T-cell clonotypes. Thus, clonotypic diversity was mostly found within the “effector-memory” EM28⁺ subset, whereas a selection was observed with advanced differentiation as certain clonotypes were enriched, while others were not. This process is likely clonotype-dependent, consistent with studies on T-cells specific for persistent viruses (5, 7), and highlighting the importance of the structural composition of the TCR repertoire for T-cell differentiation. Moreover, many tumor-specific clonotypes identified in the late-differentiated “effector-like” subset were also found within the pool of less-differentiated “effector-memory” cells, albeit at much lower frequencies. Co-

existence of identical clonotypes as both “effector-memory” and “effector-like” T-cells has also been described for human T-cells specific for influenza matrix protein peptide (16) and HIV epitopes (7). Together, these observations are in line with recent findings (17), showing that individual naive T-cells have multiple fates and can differentiate into both memory and effector T-cell subsets.

Our single cell analysis confirmed that vaccination with native peptide was more efficient at inducing the expression of multiple effector molecules, and shows that this occurred in nearly all Melan-A-specific T-cell clonotypes. This correlated with efficient target cell killing. Consequently, both T-cell subsets (EM28+ and EM28-) induced by native-peptide vaccination closely resembled each other, and to the highly differentiated CMV-specific T-cells. These data refine our current view of the process of T-cell differentiation, as they indicate that progressive up-regulation of cytolytic activity does not necessarily require the stepwise loss of costimulatory (CD27, CD28) and cytokine receptor (IL-7R α) expression. Previous reports have described a hierarchical order of T-cell differentiation stages, from naïve to CM, EM28+, EM28- and EMRA cells (12, 18-20). Specifically, it was shown that cellular differentiation (loss of CCR7/CD27/CD28 expression) was associated with progressive up-regulation of multiple “killer” mediators by the same cell (12). This report, together with our own observations (20), demonstrated tight correlations between particular cell surface markers (e.g. CCR7 $^{+/-}$, CD28 $^{+/-}$, and CD27 $^{+/-}$) and T-cell functional properties. While these studies were performed on circulating “bulk” CD8 T-cells irrespective of antigen-specificity, an alternative picture became apparent when assessing virus antigen-specific T-cells. Indeed, despite showing distinct expression patterns along with cell differentiation, CMV-specific cells also expressed globally higher levels of CD94, CD57, IFN- γ , perforin and granzyme B

than EBV-specific cells (6). The reasons behind this higher degree of differentiation and TCR clonotypic repertoire restriction are not fully understood. For example, it could be influenced by the differences in the biology of these viruses (21). Nevertheless, the fact that enhanced effector functions can be acquired without losing expression of CD27, CD28 and IL-7R α is likely important, since these receptors contribute significantly to memory cell function, essential for protection from disease.

Unfortunately, it still remains unknown why the native peptide induced qualitatively better T-cell responses than the analog peptide. We still favor the hypothesis that the native peptide recruited T-cells with superior TCR affinity/avidity, selected to overcome the lower peptide binding to MHC (the analog peptide binds about 10 times more stably to HLA-A2 than the native peptide (22)). Alternatively, vaccination with weak antigens may induce more profound T-cell activation through non-TCR mediated signals, e.g. enhanced co-stimulatory and/or reduced inhibitory pathways that are maintained in T-cell progeny. Therefore we are currently analyzing additional T-cell properties. Our preliminary data revealed relatively similar expression of the inhibitory receptors TIM-3, PD-1, CD160, CTLA-4 and BTLA among tumor-specific T-cells induced by native and analog peptide vaccination (Fig. S3 and S5).

In the future, it will be important to clarify which of the observed properties are already present before vaccination. T-cells from healthy individuals should be analyzed in parallel, before and after vaccination. However, these are major challenges, since clinical studies in healthy individuals are difficult to conduct. Furthermore, the frequencies of tumor-specific T-cells are very low in non-vaccinated

individuals, or after vaccination without CpG-ODN, even in melanoma patients, thus severely limiting direct *ex vivo* analysis.

We conclude that non-dominant clonotypes may display similar functions as their dominant counterparts, both for tumor- and virus-specific T-cells. High-resolution characterization of individual T-cells at the clonotype level provides the basis to identify the biological benchmarks associated with protective T-cell immunity, contributing to the rational development of vaccines.

MATERIALS AND METHODS

Patients and healthy blood donors. Fifteen HLA-A*0201-positive patients with stage III/IV metastatic melanoma were included in a phase I prospective trial of the Ludwig Institute for Cancer Research and the Multidisciplinary Oncology Center, approved by institutional review boards and regulatory agencies (9, 10). Patients received monthly low-dose vaccinations injected subcutaneously with 100 µg of either the Melan-A^{MART-1}₂₆₋₃₅ unmodified native peptide (EAAGIGILTV) or the Melan-A^{MART-1}₂₆₋₃₅ analog A27L peptide (ELAGIGILTV), mixed with 0.5 mg CpG-ODN 7909 / PF-3512676 (Pfizer and Coley Pharmaceutical Group) and emulsified in Incomplete Freund's Adjuvant (IFA) (Montanide ISA-51; Seppic) (9). Leukapheresis from two healthy donors (BCL6 and BCL8) with positive EBV- and CMV-specific CD8 T-cell responses were collected upon informed consent.

Cell preparation and flow cytometry. Samples were collected and processed as described in the *SI Text*. Purified CD8 T-cells were stained with HLA-A2/peptide multimers and then with appropriate mAbs, and sorted into defined sub-populations on a FACSVantage SE or a FACSaria (BD Biosciences, San Diego, CA) or immediately analyzed on a LSR IITM flow cytometer (BD Biosciences), using CellQuest (BD Biosciences) or FlowJo (TreeStar) software.

Generation of T-cell clones and functional cytolytic assays. HLA-A2/multimer+ CD8+ T-cell subsets (EM28+, EM28-, and EMRA) were sorted by flow cytometry, cloned by limiting dilution, and expanded as described in the *SI Text*. Tumor cell killing and efficiency of antigen recognition by in vitro generated T-cell clones was analyzed as detailed in the *SI Text*.

cDNA preparation, gene expression and TCR BV analysis. cDNA preparation, cDNA amplification and PCR were performed on individually sorted single-cell samples as described in the *SI Text*. 10^5 cells from T-cell clones were processed through direct lysis and cDNA synthesis without undergoing the global cDNA amplification procedure. Specific PCR reactions and TCR BV CDR3 spectratyping, sequencing and clonotyping were performed as detailed in the *SI Text*. The term “dominant clonotype” refers to a nucleotide sequence found at least twice in a given patient and time-point (> 1% of frequency) (23).

ACKNOWLEDGEMENTS

We are obliged to the patients and blood donors for their dedicated collaboration in this study, and Pfizer and Coley Pharmaceutical Group for providing CpG-ODN PF-3512676/7909. We gratefully acknowledge V. Appay, L. Derré, E. Devedre, P. Guillaume, C. Jandus, A. Legat, S. Leyvraz, T. Lövgren, I. Luescher, D. Price, and V. Voelter for essential collaboration and advice. We are also thankful for the excellent help of C. Beauverd, C. Geldhof, N. Montandon, and M. van Overloop.

This study was sponsored and supported by a grant from the Wilhelm Sander Foundation, the Swiss National Center of Competence in Research (NCCR) Molecular Oncology, the Ludwig Institute for Cancer Research, NY USA, and the Swiss National Science Foundation grant 3200B0-118123.

REFERENCES

1. Romero P, *et al.* (2002) Antigenicity and immunogenicity of Melan-A/MART-1 derived peptides as targets for tumor reactive CTL in human melanoma. *Immunol Rev* 188:81-96.
2. Boon T, Coulie PG, Van den Eynde BJ, & van der Bruggen P (2006) Human T cell responses against melanoma. *Annu Rev Immunol* 24:175-208.
3. Rufer N (2005) Molecular tracking of antigen-specific T-cell clones during immune responses. *Curr Opin Immunol* 17(4):441-447.
4. Speiser DE, *et al.* (2006) A novel approach to characterize clonality and differentiation of human melanoma-specific T cell responses: spontaneous priming and efficient boosting by vaccination. *J Immunol* 177(2):1338-1348.
5. Price DA, *et al.* (2005) Avidity for antigen shapes clonal dominance in CD8+ T cell populations specific for persistent DNA viruses. *J Exp Med* 202(10):1349-1361.
6. Iancu EM, *et al.* (2009) Clonotype selection and composition of human CD8 T cells specific for persistent herpes viruses varies with differentiation but is stable over time. *J Immunol* 183(1):319-331.
7. Meyer-Olson D, *et al.* (2010) Clonal expansion and TCR-independent differentiation shape the HIV-specific CD8+ effector-memory T-cell repertoire in vivo. *Blood* 116(3):396-405.
8. Derre L, *et al.* (2007) In Vivo Persistence of Codominant Human CD8+ T Cell Clonotypes Is Not Limited by Replicative Senescence or Functional Alteration. *J Immunol* 179(4):2368-2379.

9. Speiser DE, *et al.* (2005) Rapid and strong human CD8+ T cell responses to vaccination with peptide, IFA, and CpG oligodeoxynucleotide 7909. *J Clin Invest* 115(3):739-746.
10. Speiser DE, *et al.* (2008) Unmodified self antigen triggers human CD8 T cells with stronger tumor reactivity than altered antigen. *Proc Natl Acad Sci U S A* 105(10):3849-3854.
11. Barbey C, *et al.* (2007) IL-12 controls cytotoxicity of a novel subset of self-antigen-specific human CD28+ cytolytic T cells. *J Immunol* 178(6):3566-3574.
12. Monteiro M, Evaristo C, Legrand A, Nicoletti A, & Rocha B (2007) Cartography of gene expression in CD8 single cells: novel CCR7- subsets suggest differentiation independent of CD45RA expression. *Blood* 109(7):2863-2870.
13. Peixoto A, *et al.* (2007) CD8 single-cell gene coexpression reveals three different effector types present at distinct phases of the immune response. *J Exp Med* 204(5):1193-1205.
14. Flatz L, *et al.* (2011) Single-cell gene-expression profiling reveals qualitatively distinct CD8 T cells elicited by different gene-based vaccines. *Proc Natl Acad Sci U S A* 108(14):5724-5729.
15. Messaoudi I, Guevara Patino JA, Dyall R, LeMaout J, & Nikolich-Zugich J (2002) Direct link between mhc polymorphism, T cell avidity, and diversity in immune defense. *Science* 298(5599):1797-1800.
16. Touvrey C, *et al.* (2009) Dominant human CD8 T cell clonotypes persist simultaneously as memory and effector cells in memory phase. *J Immunol* 182(11):6718-6726.
17. Gerlach C, *et al.* (2010) One naive T cell, multiple fates in CD8+ T cell differentiation. *J Exp Med* 207(6):1235-1246.

18. Sallusto F, Lenig D, Forster R, Lipp M, & Lanzavecchia A (1999) Two subsets of memory T lymphocytes with distinct homing potentials and effector functions. *Nature* 401(6754):708-712.
19. Appay V, *et al.* (2002) Memory CD8⁺ T cells vary in differentiation phenotype in different persistent virus infections. *Nat Med* 8(4):379-385.
20. Romero P, *et al.* (2007) Four functionally distinct populations of human effector-memory CD8⁺ T lymphocytes. *J Immunol* 178(7):4112-4119.
21. Khan N, *et al.* (2004) Herpesvirus-specific CD8 T cell immunity in old age: cytomegalovirus impairs the response to a coresident EBV infection. *J Immunol* 173(12):7481-7489.
22. Valmori D, *et al.* (1998) Enhanced generation of specific tumor-reactive CTL in vitro by selected Melan-A/MART-1 immunodominant peptide analogues. *J Immunol* 160(4):1750-1758.
23. Wieckowski S, *et al.* (2009) Fine structural variations of alpha beta TCRs selected by vaccination with natural versus altered self-antigen in melanoma patients. *J Immunol* 183(8):5397-5406.

FIGURE LEGENDS

Figure 1. Analysis of TCR BV repertoire diversity and quantification of tumor-specific T-cell clonotypes. *A*, *Ex vivo* analysis of circulating Melan-A₂₆₋₃₅ specific CD8⁺ T-cells over time in fifteen melanoma patients vaccinated with either the analog A27L-modified (n = 10) or the unmodified native (n = 5) peptide, combined with CpG-ODN and IFA. Data are expressed as percentages of CD28⁻ Melan-A-specific T-cells. *B*, cDNA pools (50-100 cells), *ex vivo* sorted from peripheral blood following vaccination with native or analog peptide, were amplified by PCR using 22 BV-specific primers, and subjected to electrophoresis. TCR BV repertoire diversity is expressed as the total number of amplified BV-CDR3-BC products of different lengths within each positive BV family. *C*, Distribution of dominant and non-dominant T-cell clonotypes within EM28⁺ and EM28⁻/EMRA T-cell subsets. Compiled data representing mean clonotypic frequencies of Melan-A specific T-cells after vaccination with the analog (n = 4 patients) or native (n = 4) peptide and T-cells specific for EBV (n = 3 healthy donors) and CMV (n = 3). Analyses were performed on large numbers of *in vitro* generated T-cell clones (n = 1487). Dominant clonotypes are defined as high ($\geq 10\%$) or low (1-9%), while non-dominant T-cell clonotypes as $< 1\%$ of epitope-specific T-cells. * $0.01 < P < 0.05$, *** $P < 0.005$ (two-tailed unpaired *t* test).

Figure 2. *Ex vivo* gene expression profiling of individually sorted T-cells. *A*, Gene expression analysis was performed on cDNA obtained from individually sorted single-cell samples isolated from EM28⁺ and EM28⁻ T-cell subsets (patients vaccinated with analog or native peptide), and from EM28⁺ and EMRA subsets (EBV- and CMV-specific T-cells from the healthy individual BCL8). Positive PCR

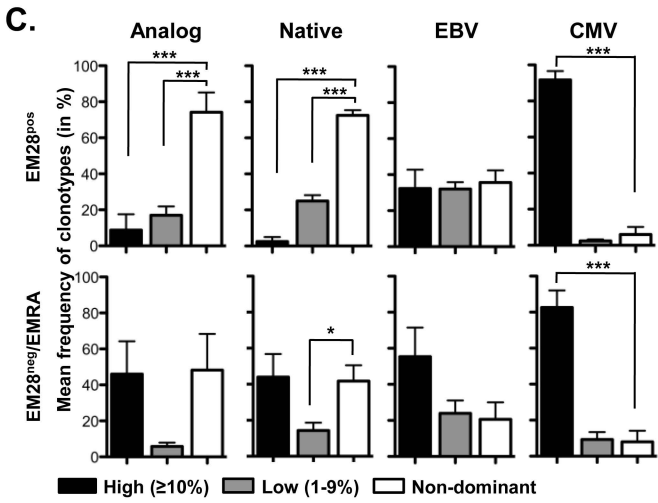
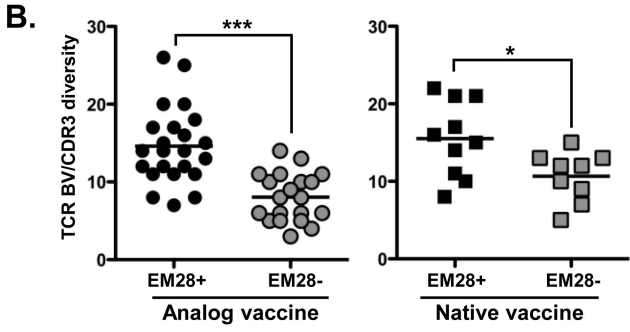
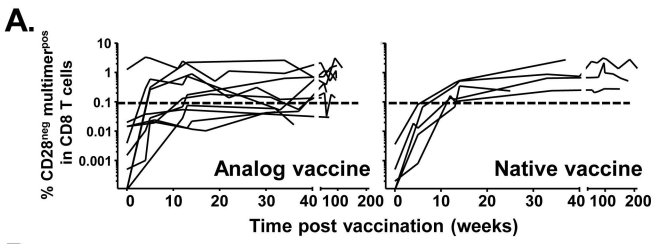
products are depicted in red, negative ones in blue. Compiled data are shown per subset and per patient/healthy individual, where each line represents an individual T-cell. *B*, Complete sets of data of the proportion of each expressed gene in early- (EM28+) or late- (EM28-/EMRA) differentiated subsets from four patients vaccinated with analog (LAU 618, ●; LAU 672, ■) and native peptide (LAU 1013, ○; LAU 972, □), and from two healthy donors BCL8 (EBV, ▲; CMV, ◆) and BCL6 (CMV, ▼). *C*, A hierarchical clustering (*left panel*) ($n = 529$ single-cell samples) was performed based on Euclidean distance between samples with the UPGMA clustering method (as described in *SI Text*) and allowed the identification of 5 distinct clusters. The repartition of these clusters within the single-cell samples of each EM28+ and EM28- T-cell subset (specific for ELA, EAA, EBV or CMV) was determined by Heat-map analysis (*right panel*).

Figure 3. *Ex vivo* expression of effector proteins within tumor- and virus-specific CD8 T-cell subsets by multi-parameter flow cytometry. The proportion of CD57, perforin and granzyme B protein expression was determined within antigen-specific EM28+ and EM28- T-cell subsets from fifteen melanoma patients following analog (ELA, $n = 10$) or native (EAA, $n = 5$) peptide vaccination, and from seven healthy individuals with EBV ($n = 5$) and/or CMV ($n = 5$) specific T-cell responses. * $0.01 < P < 0.05$, ** $0.005 < P < 0.01$, *** $P < 0.005$ (two-tailed unpaired *t* test).

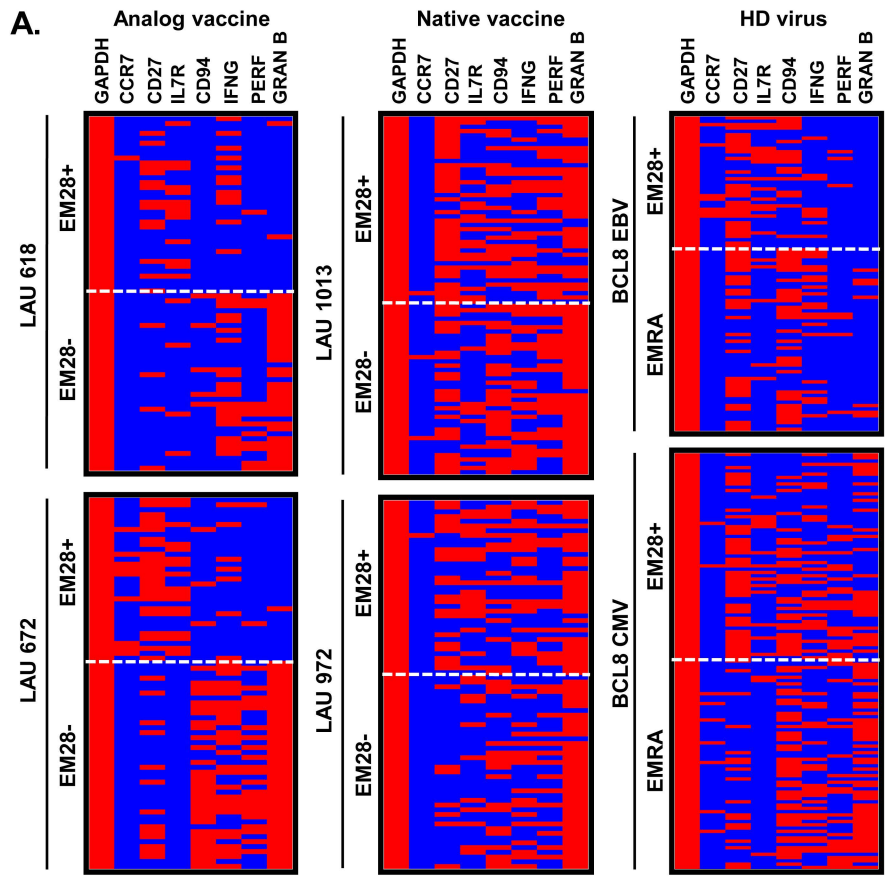
Figure 4. Co-expression of effector molecules by T-cell clonotypes. Poly-functional gene expression profile was determined for dominant (*A*) and non-dominant (*B*) tumor- and virus-specific T-cell clonotypes, upon *ex vivo* single-cell sorting of EM28+ and EM28-/EMRA T-cells. Dominant clonotypes (*A*) are defined according

to their relative frequencies in epitope specific T-cell subsets as high (> 10 %) or intermediate (1-9 %), and non-dominant TCRs (*B*) as frequencies < 1%. The pie charts illustrate co-expression of *CD94*, *IFN- γ* , *perforin* and *granzyme B* as detected in single-cell samples from four patients vaccinated with the analog (n = 2) and the native (n = 2) peptide and two healthy individuals.

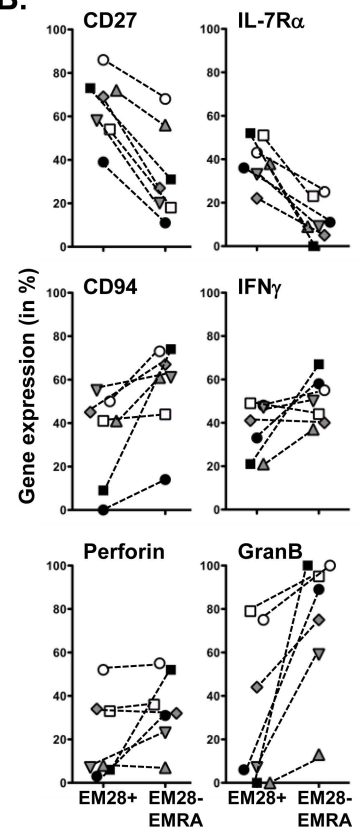
Figure 5. Tumor cell killing and efficiency of antigen recognition. Tumor-specific T-cell clones were *in vitro* generated from four patients following analog (n = 2) or native (n = 2) peptide vaccination. *A*, Tumor reactivity for melanoma cell lines Me290 (A2+/Melan-A+) and NA8 (A2+/Melan-A-) in the absence or presence of synthetic Melan-A analog peptide (1 μ M), at an effector:target ratio of 30:1. Each line represents an individual clone derived from EM28+ and EM28- subsets after analog (n = 153) or native (n = 80) peptide vaccination. *B*, Complete set of data representing specific lysis of the Melan-A+ Me290 tumor cell line without exogenous peptide (effector:target ratio; 10:1) by T-cell clones derived from EM28+ and EM28- subsets following analog (n = 2 patients; grey whiskers) or native (n = 2; empty whiskers) peptide vaccination. To allow direct comparison, clones were divided into dominant (frequencies > 1%) and non-dominant (frequencies < 1%) subgroups. ** $0.0001 < P < 0.001$, *** $P < 0.0001$ (two-tailed unpaired *t* test).



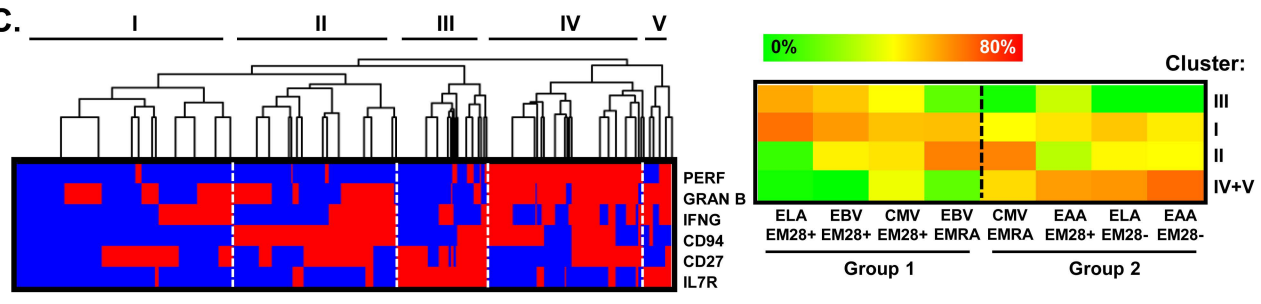
A.

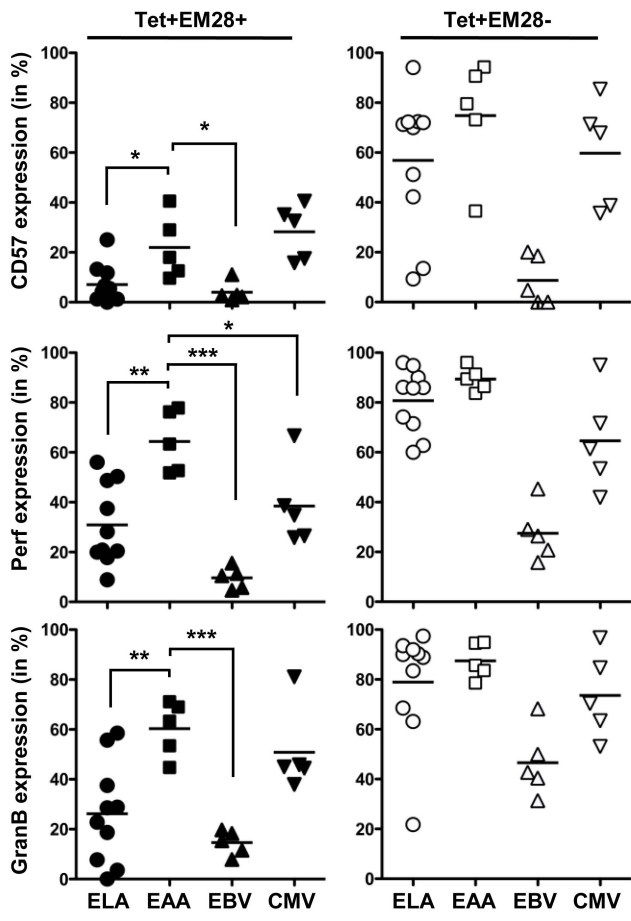


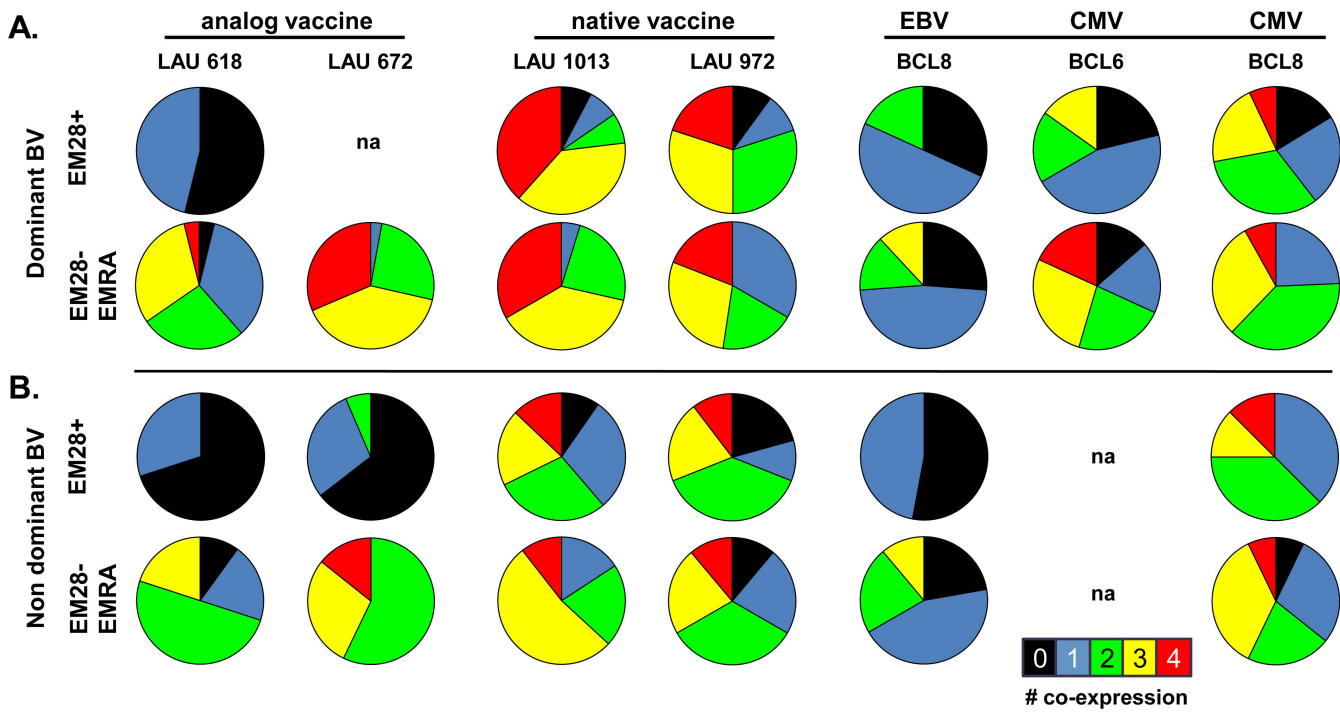
B.

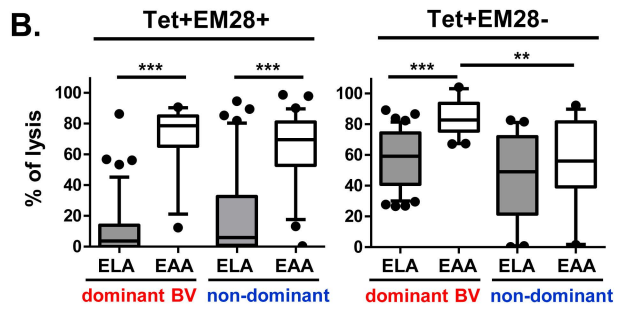
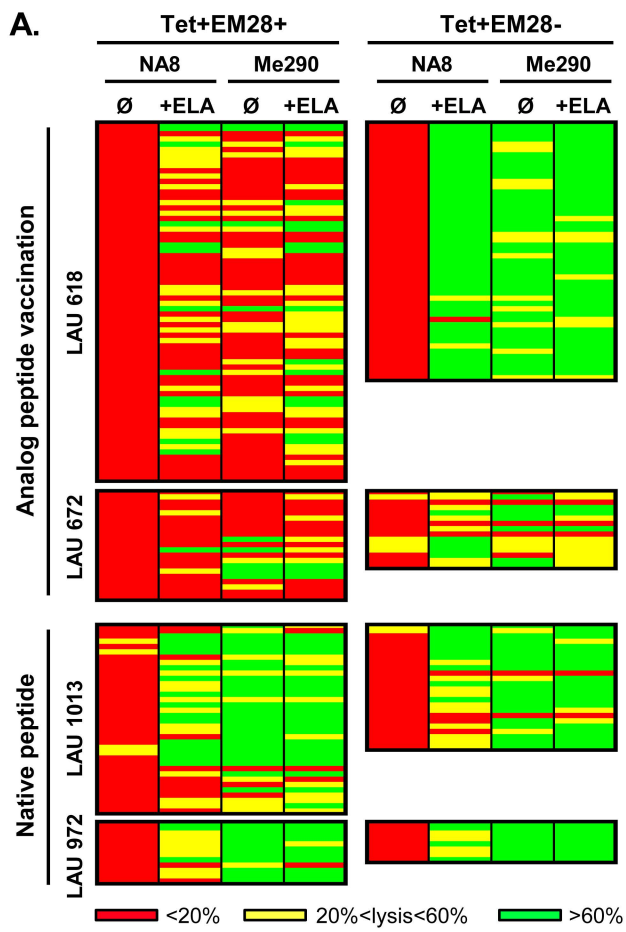


C.









SUPPORTING MATERIAL AND METHODS

Patients. HLA-A2-positive patients with histological proven metastatic (stage III/IV) melanoma expressing Melan-A (RT-PCR or immuno-histochemistry) were included upon written informed consent, as described previously (1, 2). The following inclusion criteria had to be fulfilled: Karnofsky performance status of 70%, normal CBC and kidney-liver function, no concomitant anti-tumor therapy nor immunosuppressive drugs. Exclusion criteria were pregnancy, seropositivity for HIV-1 Ab or HBs Ag, brain metastases, uncontrolled bleeding, clinically significant autoimmune disease, and symptomatic heart disease (NYHA III-IV). Study end points were toxicity and CD8 T-cell responses.

Cell preparation, antibodies, and flow cytometry. Ficoll-Paque centrifuged peripheral blood mononuclear cells (PBMCs) were cryopreserved in RPMI 1640, 40% FCS and 10% DMSO. Synthesis of phycoerythrin (PE)-labeled HLA-A*0201/peptide multimers with A27L Melan-A^{MART-1}₂₆₋₃₅ (ELAGIGILTV), EBV BMLF1₂₈₀₋₂₈₈ (GLCTLVAML), and CMV pp65₄₉₅₋₅₀₃ (NLVPMVATV) was prepared as described previously (3). Before staining, CD8^{pos} T-cells were positively enriched using a MiniMACS device (Miltenyi Biotech, Bergish Gladbach, Germany) resulting in > 90% CD3^{pos}CD8^{pos} cells. Cells were stained in PBS, 0.2% BSA, 50 μ M EDTA with multimers (1 μ g/ml, 60 min, 4°C), and sorted into defined sub-populations on a FACSVantage SE or a FACS Aria (BD Biosciences, San Diego, CA) or immediately analyzed on a LSR IITM flow cytometer (BD Biosciences), using CellQuest (BD Biosciences) or FlowJoTM (TreeStar) software. For dead cell exclusion, cells were stained with Live/Dead Fixable Dead Cell violet stain (Molecular Probes / Invitrogen). Extracellular and intracellular stainings were performed according to the manufacturer's instructions. Manipulations were done at 4°C, avoiding gene expression alteration due to staining and sorting procedures.

All flow cytometry-based sorting experiments (*ex vivo* single-cell aliquots, and *in vitro* generation of T-cell clones) were performed using the following 5-color stain combination: (a) PE-HLA-A2/peptide multimers, (b) FITC-conjugated anti-CD28 (BD Biosciences), (c) PE-Texas Red-conjugated anti-CD45RA (Beckman Coulter), (d) APC-

Cy7-conjugated anti-CD8 (BD Biosciences) reagents and (e) anti-CCR7 mAb (BD Biosciences) followed by APC-conjugated goat anti-rat IgG Ab (for indirect staining for CCR7) (Caltag Laboratories).

Multi-parameter flow cytometry analyses were performed using the following 8-color stain strategy: (a) PE-HLA-A2/peptide multimers, (b) FITC-conjugated anti-CD57 (BD Biosciences) or -PD1 (BD Biosciences) or -Granzyme B (Hölzer Diagnostic) or -Perforin (Ancell), (c) PE-Texas Red-conjugated anti-CD45RA (Beckman Coulter), (d) PE-Cy7-conjugated CCR7 (BD Biosciences), (e) Alexafluor700 anti-CD28 (Biolegend), (f) Pacific Blue-labeled anti-CD8, (g) PerCP-Cy5.5 anti-CD127 (IL-7R) (Beckman Coulter), and (h) APC-eFluor780-conjugated anti-CD27 (eBioscience) mAbs.

For antibody staining of inhibitory receptors, samples were purified and enriched for CD8^{pos} T-cells, and then stained using Melan-A^{MART-1} multimers as described above. Melan-A-specific multimers were labeled with APC-eFluor 780 (eBioscience) and after 45 min at 4°C, cells were washed and surface staining was performed for CD8, CCR7, CD45RA, and (a) 2B4 (PE-Cy5.5; BioLegend) and BTLA (PE; BD Biosciences) or (b) KLRG-1 (Alexa Fluor 488; a gift from H.-P. Pircher, Department of Immunology, University of Freiburg, Freiburg, Germany), TIM-3 (PE; R&D Systems), and CD160 (Alexa Fluor 647; eBioscience) as described elsewhere (4). Samples (a) were fixed at room temperature for 30 min (1% formaldehyde buffer) and then stained for CTLA-4 (APC; BD Biosciences) in FACS buffer for 0.1% saponin for 30 min at 4°C. Live/Dead Fixable Aqua (Invitrogen) was used as dead cell exclusion marker, and appropriate isotype controls were used to define negative populations. Data were acquired on a GalliosTM Flow Cytometer (Beckman Coulter) analyzed using FlowJoTM (TreeStar).

For intracellular cytokine (IFN- γ) and degranulation (CD107a/LAMP1) analyses, cells were kept overnight in RPMI 10% FCS at 37°C and 5% CO₂. CD8^{pos} T-cells were enriched as described above, and purified CD8^{pos} T-cells were first pre-stained with PE-labeled multimers for 30 min at 4°C. 4×10^5 T-cells were incubated with 2×10^5 T2 cells at 37°C for 4h with or without 10 μ M peptide (Melan-A/MART-1 ELAGIGILTV) and anti-CD107a^{FITC} (BD Biosciences), whereby 10 μ g/ml Brefeldin A (Sigma, St. Louis, MO) was added for the last 3h, in culture medium consisting of RPMI supplemented with 0.55 mM Arg, 0.24 mM Asn, 1.5 mM Gln, and 8 % pooled human A^{pos} serum. Subsequently, cells were stained at 4°C with PE-labeled multimers, anti-CD8, anti-CD28 and anti-CD45RA antibodies. For dead cell exclusion, cells were stained with Live/Dead Fixable

Dead Cell violet stain (Invitrogen). Then, cells were permeabilized with 0.1 % saponin at 4°C, washed, and stained for 40 min with anti-IFN γ ^{Pe-Cy7} (BD Biosciences). CD8^{pos} T-cells were acquired with a flow cytometry LSR IITM machine, and analyzed with FlowJoTM software (TreeStar). Data are indicated in percentages of circulating CD8^{pos} T-cells.

Generation of T-cell clones. HLA-A2/multimer^{pos} CD8^{pos} T-cell subsets (EM28^{pos}, EM28^{neg}, and EMRA) were sorted by flow cytometry, cloned by limiting dilution and expanded in RPMI 1640 medium supplemented with 8% human serum, 150 U/ml recombinant human IL-2 (rhIL-2; a gift from GlaxoSmithKline), 1 μ g/ml phytohemagglutinin (PHA; Sodiag, Losone, Switzerland) and 1 \times 10⁶/ml irradiated allogeneic PBMC (3000 rad) as feeder cells. T-cell clones were expanded by periodic (every 15 days) restimulation with PHA, irradiated feeder cells, and rhIL-2.

Direct cell lysis and cDNA synthesis. Single-cell or five-cell aliquots were sorted by flow cytometry directly into 96-V bottom plates containing 15 μ l of a lysis/cDNA mix solution supplemented with 1.2% Triton X-100 (Fluka), 30 μ g/ml tRNA (Roche), 10 mM DTT (Fluka), 0.5 mM dNTP (Invitrogen, Paisley, UK), 2 ng/ μ l of a 20-mer oligo-dT (Amplimmun, Madulain, Switzerland), 4 U of RNAsin (Promega, Madison, WI), 3 μ l of RT buffer (5x; Invitrogen) and 40 U of M-MLV transcriptase (Invitrogen), as described in detail elsewhere (5). To allow the transcription of total mRNA into cDNA, the 96-well plates were incubated 60 min at 37°C, briefly centrifuged and transferred into 0.5 ml PCR tubes. MMLV-RT transcriptase was inactivated at 90°C for 3 min and samples were stored at -80°C until further use. For T-cell clones, 15 μ l of lysis/cDNA mix was directly added to 10⁵ cells and further processed as described above.

Global cDNA amplification from single-cells. The basic principle of the five-cell and single-cell global cDNA amplification protocol requires that the target sequences to be amplified be flanked by known sequences to which the amplification primers can anneal and initiate polymerization. One end is initially defined through a cDNA reaction using reverse transcriptase and an oligo(dT) primer that will prime via the poly(A) tail present at the 3' end of most mRNA molecules. The other end is then created by the addition of

an homopolymer d(A) sequence to the 3'-OH end of the first cDNA using terminal deoxynucleotidyl transferase. Global PCR amplification of the dA/dT flanked cDNAs is carried out using a single modified oligo(dT) primer as previously described by Brady and Iscove (6). Priming of the cDNA during global RT-PCR is initiated via annealing of the d(T) region of the 61-mer oligonucleotide primer to the homopolymeric d(A) regions present at the termini of the cDNA molecules. We have included a purification step before adding the poly d(A) tails, in order to get rid of free dNTPs that may interfere during the tailing reaction. Therefore, for further processing, cDNA from single-cell or five-cell aliquots were precipitated overnight at -20°C after addition of 7.5 µl of C₂H₇NO₂ 7.5 M (Fluka), 45 µl of ethanol 100% (Fluka) using 2 µl of Glycogen 10 mM (Roche) as carrier, washed in 150 µl of cold ethanol 70% and dried 1 hour at room temperature.

To evaluate mRNA expression in small numbers of cells (single or five-cell sorted samples), the following method was adapted from previously published protocols (6, 7). Briefly, to allow 3'oligo(dA) tailing to cDNA, the dried pellets were suspended in 5 µl of tailing solution containing 0.5 mM dATP (Amersham Pharmacia), 1 U of Terminal deoxynucleotidyl Transferase (Promega) and 1 µl tailing buffer (5x; Promega) and incubated at 37°C for 30 min. After denaturation (94°C for 3 min), 45 µl of PCR-buffer (10 mM Tris-HCl pH 8.8, 50 mM KCl, 0.1 mg/ml BSA, 2 mM MgCl₂) containing 20 ng/µl of a 61-mer oligo dT (5'-CATGTCGTCCAGGCCGCTCTGGGACAAAATATG AATTCT₂₃-3') (Metabion), 0.2 mM dNTP, 0.5% Triton X-100, and 5 U Taq DNA recombinant polymerase Platinum (Invitrogen) were added, followed by 5 cycles of PCR (50s at 94°C; 2 min at 37°C; 9 min at 72°C) and of 35 cycles (50s at 94°C; 90s at 60°C; 8 min at 72°C). 1 µl of amplified cDNA (also defined as cDNA^{plus}) was then subjected to a second round of PCR amplification (38-40 cycles, 30s at 94°C; 45s at 58°C; 1 min at 72°C) in 20 µl volumes of 1x PCR buffer containing 1.5 mM MgCl₂, 0.2 mM dNTP, 0.5 U Taq Platinum and 40 ng of specific primers designed to amplify mRNA sequences of interest and the expected products were visualized after electrophoresis on a 1.2% agarose gel. Typically, we used H₂O for the negative PCR control, while 10³ PBMCs from a healthy individual were used as positive PCR control.

Gene expression analysis. For gene expression analysis of single cells, we used the following primers: *CD3*: 5'-CGTTCAGTTCCCTCCTTTTCTT-3'; rev-5'-GATTAGGGGGTTGGTAGGGAGT G-3', *GAPDH*: 5'- GGACCTGACCTGCCGTC TAG-3'; rev-5'-CCACCACCCTGTTGCTGTAG-3', *CCR7*: 5'-CCAGGCCTTATCTCC AAGACC-3'; rev-5'-GCATGTCATCCCCACTCTG-3', *CD27*: 5'-ACGTGACAGAGT GCCTTTTCG-3'; rev-5'-TTTGCCCGTCTTGTAGCATG-3', *CD127/IL-7Ra*: 5'-ATC TTGGCCTGTGTGTTATGG-3'; rev-5'-ATTCTTCTAGTTGCTGAGGAAACG-3'; *CD94*: 5'-GTGGGAGAATGGCTCTGCAC-3'; rev-5'-TGAGCTGTTGCTTACAGA TATAACGA-3', *IFN- γ* : 5'-GCCAACCTAAGCAAGATCCCA-3'; rev-5'-GGAAGC ACCAGGCATGAAATC-3', *Perforin*: 5'-TT CACTGCCACGGATGCCTAT-3'; rev-5'-GCGGAATTTTAGGTGGCCA-3', *Granz B*: 5'-GCAGGAAGATCGAAAGTGCGA-3'; rev-5'-GCATGCCATTGTTTCGTCCAT-3'. All *ex vivo* single-cell cDNA samples were processed with the same rigorous approach to allow direct comparison among individuals and subsets.

TCR spectratyping, sequencing and clonotyping. To rapidly identify TCR V β segment usage, a small fraction (5 μ l of a total of 50 μ l) from 10 individually sorted and amplified 5-cell cDNA samples were pooled and subjected to individual PCR in non-saturating conditions using a set of previously validated fluorescent-labeled forward primers specific for the 22 TCR V β subfamilies and one unlabeled reverse primer specific for the corresponding C gene segment (8, 9). This TCR V β -CDR3 spectratyping analysis based on the equivalent of 50 cells represents a pre-screening step. Once positive TCR V β subfamilies were identified, the following step consisted in subjecting each individually generated single-cell or five-cell cDNA sample, and in parallel *in vitro* generated T-cell clone to TCR V β PCRs. Separation and detection of amplified fragments that contain the entire CDR3 segment was performed in the presence of fluorescent size markers on an ABI PRISM 310 Genetic Analyzer (AppliedBiosystems, Rotkreuz, Switzerland) according to the manufacturer's recommendations, and data were analyzed with GeneScan 3.7.1 (AppliedBiosystems). In the last step, PCR products of interest were directly purified and sequenced from the reverse primer (Fasteris SA, Plan-les-Ouates, Switzerland). Clonotypic primers for several CDR3 sequences were validated and used in clonotypic PCR for determination of clonotype frequencies as previously reported (10, 11). All *ex vivo* single-cell or *in vitro* T-cell clone cDNA samples were processed with

the same rigorous approach to allow direct comparison among individuals and subsets.

Hierarchical clustering analyses. Hierarchical agglomerative clustering and dendrogram display of gene expression data were performed with HCE (Hierarchical Clustering Explorer) version 3.5 (<http://www.cs.umd.edu/hcil/hce/>). All PCR results were encoded into a data matrix in which the assigned value was +1 for a positive PCR product and 0 for a negative PCR product. The data were examined without normalization/transformation using Euclidean distance with the Unweighted Pair Group Mean Arithmetic (UPGMA) clustering method. The cluster dendrogram identified 5 distinct clusters (minimum similarity set to 0.375). Control genes (*GAPDH* and *CCR7*) were not included during clustering analysis.

Chromium release and tumor recognition assays. Lytic activity and antigen recognition was assessed functionally in 4-h ^{51}Cr -release assays using T2 target cells (HLA-A*0201⁺/Melan-A⁻) pulsed with serial dilutions of the native Melan-A^{MART-1}₂₆₋₃₅ peptide (EAAGIGILTV) or of the analog Melan-A^{MART-1}₂₆₋₃₅ A27L (ELAGIGILTV) (12). The percentage of specific lysis was calculated as $100 \times (\text{experimental} - \text{spontaneous release}) / (\text{total} - \text{spontaneous release})$. Similarly, the specific antigen recognition lytic activity of the Melan-A^{MART-1}-specific T-cell clonotypes was assessed against the melanoma cell lines NA8 (HLA-A2⁺/Melan-A⁻) and Me 290 (HLA-A2⁺/Melan-A⁺) in the presence or absence of the indicated peptide at the indicated concentration.

SUPPORTING FIGURE LEGENDS

Figure S1. (A) Analysis of relative frequencies of public T-cell clonotypes within Melan-A-specific T-cells. Graphs summarize the distribution of the public amino acid TCR β -domain sequences detected in fifteen melanoma patients vaccinated either with the analog (n = 10) or the native (n = 5) peptide vaccine, according to their relative frequency. Non-dominant clonotypes (< 1% of tumor-specific T-cells) are represented in white, low dominant (1-9%) are in gray, and high dominant (with frequency > 9%) are in black. These public TCR BV sequences were equivalently distributed within the two cohorts of vaccinated patients. The majority of these TCR BV public sequences were largely present as non-dominant or as low dominant sequences in individual patients (> 90%), but they were recurrent as they are found in various patients. Importantly, only a minority of public clonotypes (between 3 to 6 %) was typically found at higher frequencies (also defined as dominant clonotypes). Altogether, these data indicate that public T-cell clonotypes are rather infrequent within Melan-A-specific T-cell responses of both cohorts of patients (analog and native peptide vaccination). In contrast, the dominant tumor-specific T-cell clonotypes of high frequency that expand during peptide vaccination are highly specific to individual patients as defined by their private CDR3 β sequences. **(B)** Analysis of the T-cell clonotype repertoire following sorting with multimers constructed with analog versus native peptide. Clonotypic PCR was performed on *in vitro* generated specific T-cell clones from patients LAU 618 (n = 511 clones) and LAU 972 (n = 246 clones), vaccinated respectively with the analog or the native peptide. Each dominant clonotype (frequency \geq 1%) is indicated and each TCR BV family is color-coded. Non-dominant clonotypes are designed as “BV other” and are comprised of clonotypes of unique TCR BV/CDR3 sizes and/or BV-CDR3-BC sequences as determined by capillary electrophoresis and sequencing. The frequencies/proportions of T-cell clonotypes within early-differentiated EM28^{pos} and late-differentiated EM28^{neg} T-cell subsets sorted using the analog peptide multimers is directly compared with those obtained following native peptide multimer sorting. TCR BV usage and sequences were described according to the Arden nomenclature (13). The tumor-specific TCR repertoire contained similar frequencies of dominant and non-dominant T-cell clonotypes following sorting with both multimers, thus showing a very high degree of cross-reactivity and indicating that the two multimers efficiently bound to all Melan-A-specific T-cells with similar fine specificity to analog or native peptide, in line with our previous report (2).

Figure S2. *Ex vivo* gene expression analysis of effector mediators in individually sorted Melan-A-specific T-cell subsets. **(A)** Examples of gene expression profiles in two patients vaccinated with the analog (LAU 672) or the native (LAU 972) peptide. Primers designed for GAPDH, CCR7, CD27, IL-7R α , CD94, IFN- γ , perforin and granzyme B mRNA transcripts are depicted. Data from 15 independent single-cell aliquots are shown. **(B)** The pie charts depict co-expression profiles of CD94, IFN- γ , perforin and granzyme B within individually single-cell samples from (i) tumor-specific EM28^{pos} and EM28^{neg} T-cell subsets (four melanoma patients) and (ii) virus-specific EM28^{pos} and EM T-cell subsets (two healthy donors) as described in the main manuscript. Patients vaccinated with the analog peptide are LAU 618 and LAU 672, whereas patients vaccinated with the native peptide are LAU 1013 and LAU 972. EBV-specific T-cell responses were characterized from healthy donor BCL8 and CMV-specific responses from healthy individuals BCL6 and BCL8.

Figure S3. *Ex vivo* expression of effector mediators in antigen-specific CD8 T-cell subsets by multi-parameter flow cytometry. **(A)** The proportion of CD57, perforin and granzyme B protein expression among antigen-specific EM28+ and EM28- subsets was determined by multi-parameter flow cytometry. The dotted line was set according to the gating obtained on bulk CD8+ naive T-cells known to be CD57-perforin-granzymeB-. Representative examples are shown. **(B)** The proportion of CD27, IL-7R α and PD1 protein expression was determined within EM28^{pos} and EM28^{neg} T-cell subsets from fifteen melanoma patients following analog (ELA, n = 10; grey whiskers) or native (EAA, n= 5; white whiskers) peptide vaccination, and from seven healthy individuals with EBV (n= 5; dashed grey whiskers) and/or CMV (n = 5; dashed white whiskers) specific T-cells. **(C)** Direct *ex vivo* analysis of tetramer-gated T-cells for cytokine production (IFN γ) and degranulation (CD107a/LAMP-1), after 4h incubation with peptide-pulsed T2 cells as described in the Supporting Material and Methods. Data were obtained from melanoma patients vaccinated with the analog/ELA (n = 8) and the native/EAA (n = 4) peptide. The analysis included the two subpopulations CD28^{pos} and CD28^{neg} cells. Of note, the production of IFN γ and up-regulation of LAMP-1/CD107a by tumor (Melan-A) specific T-cells were similar between both cohorts of patients (with no statistically significant differences as assessed by two-tailed unpaired *t* test).

Figure S4. Functional avidity was assessed using T2 target cells ($A2^{\text{pos}}/TAP^{\text{neg/neg}}$) pulsed with graded concentrations of analog/ELA Melan-A₂₆₋₃₅ peptide. Tumor-specific T-cell clones were *in vitro* generated from four melanoma patients following analog (n = 2) and native (n = 2) peptide vaccination as described in Supporting Material and Methods. Complete set of data representing maximal lysis (**A**) and EC_{50} (e.g. peptide concentration required to achieve 50% of maximal lysis) (**B**). Clones with undetectable lytic activity ($EC_{50} > 10^{-6}$ M and/or maximal lysis < 20%) are symbolized as single dots and were not included in the statistical evaluations. * $0.001 < P < 0.01$, ** $0.0001 < P < 0.001$, *** $P < 0.0001$ (two-tailed unpaired *t* test). (**A, B**) To allow direct comparison, clones were divided into dominant (frequencies > 1%) and non-dominant (frequencies < 1%) subgroups. Native peptide vaccination-induced T-cells derived from $EM28^{\text{pos}}$ cells were again significantly superior in regards to maximal lysis capacity, compared to the killing responses obtained from the corresponding subset upon analog peptide vaccination. Efficient maximal T2 lysis was found for both dominant and non-dominant clonotypes issued from native peptide vaccination, as well as from the $EM28^{\text{neg}}$ subsets. Regarding functional avidity (EC_{50}), all native and analog peptide-derived $EM28^{\text{pos}}$ T-cell clones behaved similarly, with 50% maximal lysis of T2 cells found at comparable peptide doses (and no statistically significant differences). Yet, T-cell clones derived following analog peptide vaccination showed a higher degree of heterogeneity where a substantial fraction of the clones depicted poor to no killing, contrasting with the native peptide vaccination-induced clones displaying more homogeneous killing capacities.

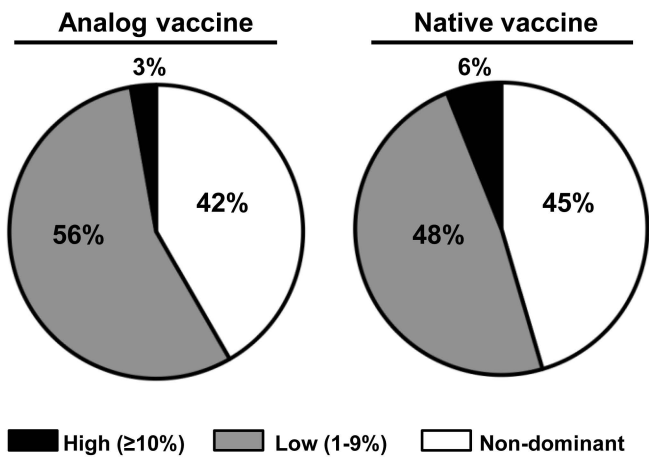
Figure S5. *Ex vivo* multimer staining assessing expression of inhibitory receptors. Tumor (Melan-A^{MART-1}) specific T-cells were analyzed for the expression of 5 different inhibitory receptors; TIM-3, KLRG-1, BTLA, CTLA-4 and CD160 as well as the 2B4 receptor as recently described (4, 14). Analysis was performed on gated on $CD8^{\text{pos}}$ multimer^{pos} T-cells from melanoma patients vaccinated either with the analog/ELA (n = 6 patients) or the native/EAA (n = 3 to 4 patients) peptide. Of note, even though many tumor-specific T-cells can express inhibitory receptors such as TIM-3, KLRG-1 and BTLA, they nevertheless also maintain functional competence (i.e. by expressing IFN- γ , perforin and granzyme B mediators and retaining killing capacities as shown in the main manuscript). In line with these observations, we recently described that while tumor-specific T-cells found within peripheral blood from melanoma patients can acquire

substantial effector cell properties, they display an exhaustion profile within metastatic lesions (4). Finally, no differential expression of inhibitory receptors was found within tumor-specific T-cells derived from patients vaccinated with the analog versus the native peptide.

REFERENCES

1. Speiser DE, *et al.* (2005) Rapid and strong human CD8+ T cell responses to vaccination with peptide, IFA, and CpG oligodeoxynucleotide 7909. *J Clin Invest* 115(3):739-746.
2. Speiser DE, *et al.* (2008) Unmodified self antigen triggers human CD8 T cells with stronger tumor reactivity than altered antigen. *Proc Natl Acad Sci U S A* 105(10):3849-3854.
3. Pittet MJ, *et al.* (1999) High frequencies of naive Melan-A/MART-1-specific CD8(+) T cells in a large proportion of human histocompatibility leukocyte antigen (HLA)-A2 individuals. *J Exp Med* 190(5):705-715.
4. Baitsch L, *et al.* (2011) Exhaustion of tumor-specific CD8+ T cells in metastases from melanoma patients. *J Clin Invest* 121(6):2350-2360.
5. Rufer N, Reichenbach P, & Romero P (2005) Methods for the ex vivo characterization of human CD8+ T subsets based on gene expression and replicative history analysis. *Methods Mol Med* 109:265-284.
6. Brady G & Iscove NN (1993) Construction of cDNA libraries from single cells. *Methods Enzymol* 225:611-623.
7. Sauvageau G, *et al.* (1994) Differential expression of homeobox genes in functionally distinct CD34+ subpopulations of human bone marrow cells. *Proc Natl Acad Sci U S A* 91(25):12223-12227.
8. Roux E, *et al.* (1996) Analysis of T-cell repopulation after allogeneic bone marrow transplantation: significant differences between recipients of T-cell depleted and unmanipulated grafts. *Blood* 87(9):3984-3992.
9. Roux E, *et al.* (2000) Recovery of immune reactivity after T-cell-depleted bone marrow transplantation depends on thymic activity. *Blood* 96(6):2299-2303.
10. Iancu EM, *et al.* (2009) Clonotype selection and composition of human CD8 T cells specific for persistent herpes viruses varies with differentiation but is stable over time. *J Immunol* 183(1):319-331.
11. Wieckowski S, *et al.* (2009) Fine structural variations of alpha beta TCRs selected by vaccination with natural versus altered self-antigen in melanoma patients. *J Immunol* 183(8):5397-5406.
12. Romero P, *et al.* (2001) CD8+ T-cell response to NY-ESO-1: relative antigenicity and in vitro immunogenicity of natural and analogue sequences. *Clin Cancer Res* 7(3 Suppl):766s-772s.
13. Arden B, Clark SP, Kabelitz D, & Mak TW (1995) Human T-cell receptor variable gene segment families. *Immunogenetics* 42(6):455-500.
14. Derre L, *et al.* (2010) BTLA mediates inhibition of human tumor-specific CD8+ T cells that can be partially reversed by vaccination. *J Clin Invest* 120(1):157-167.

A.

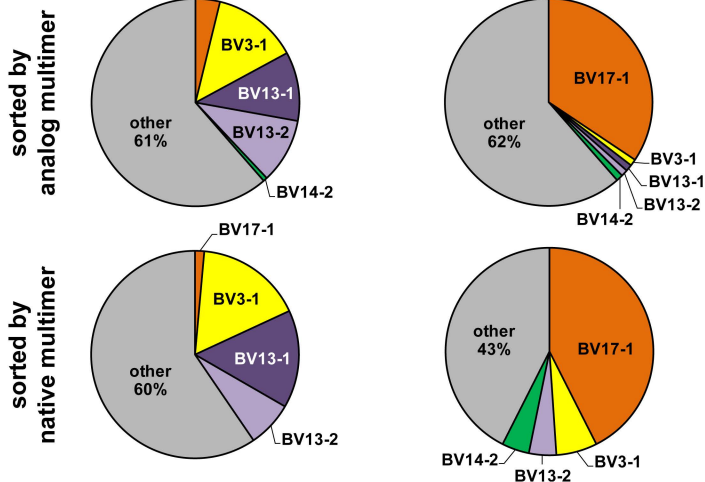


B.

LAU 618 (analog peptide vaccine)

EM28+

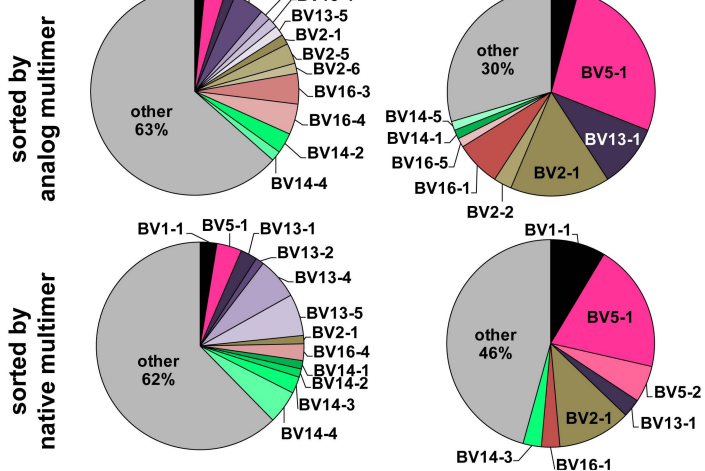
EM28-



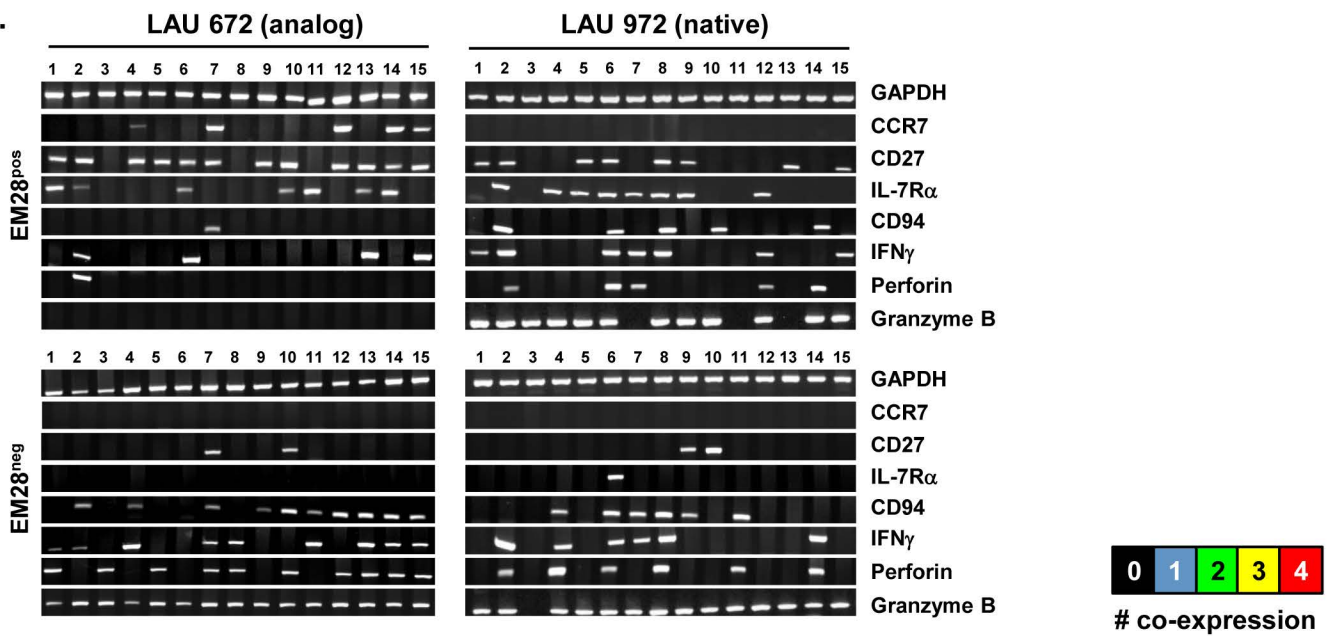
LAU 972 (native peptide vaccine)

EM28+

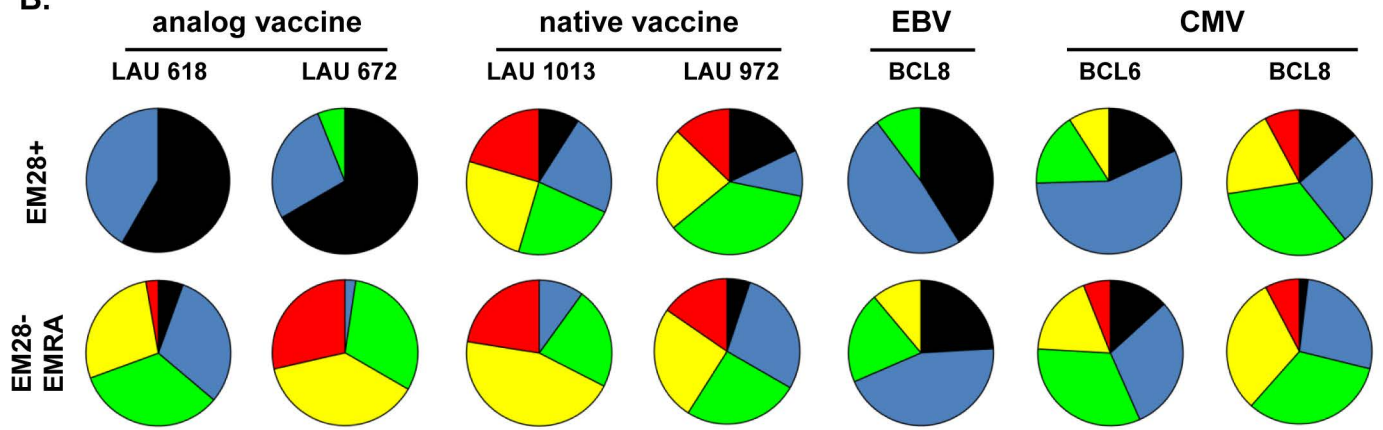
EM28-

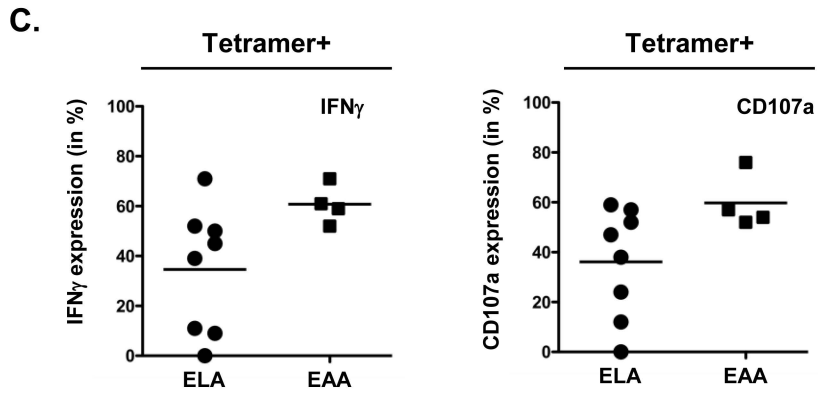
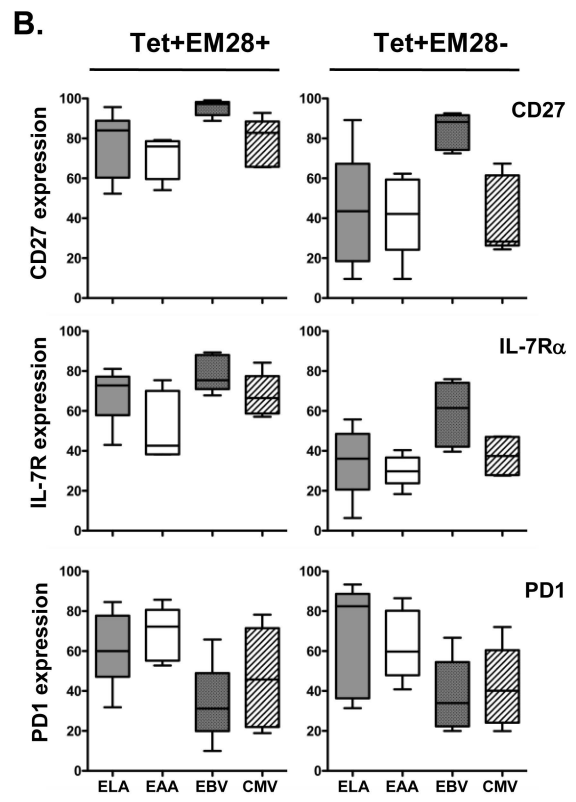
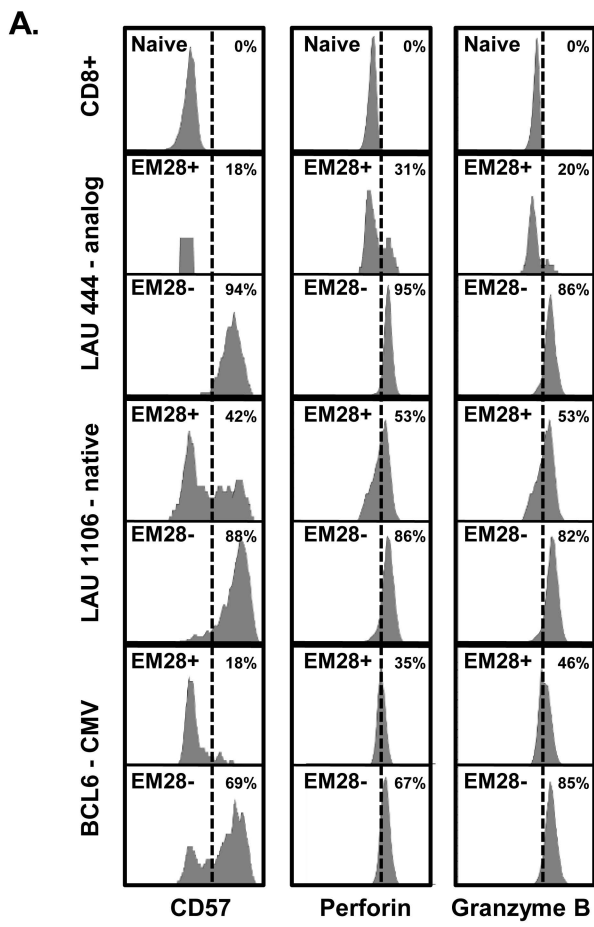


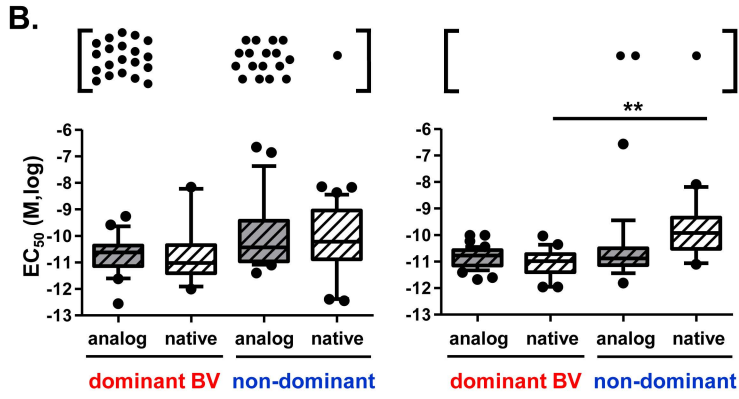
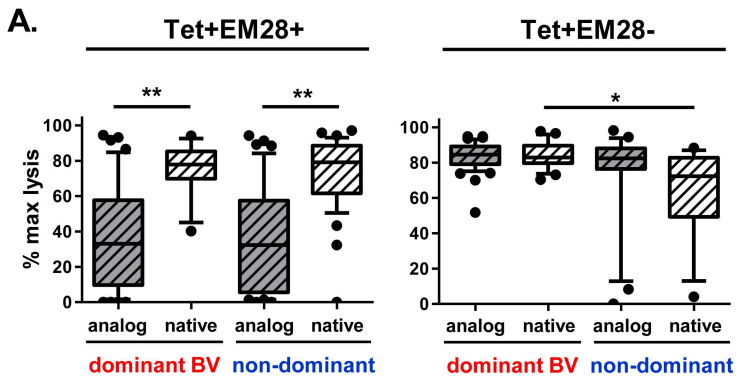
A.



B.







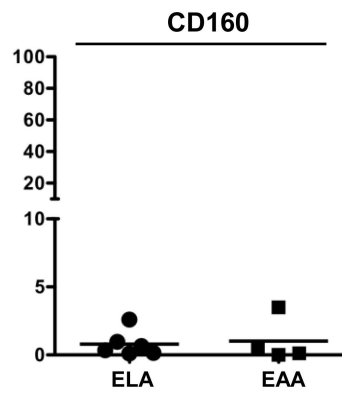
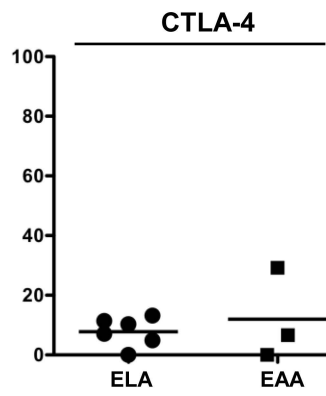
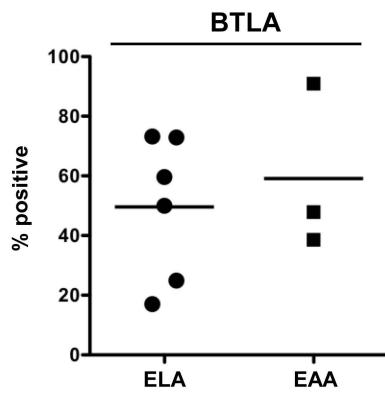
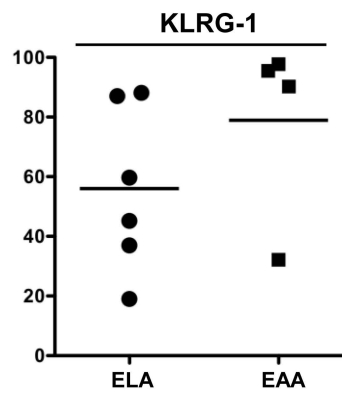
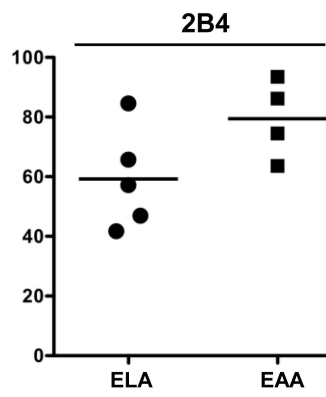
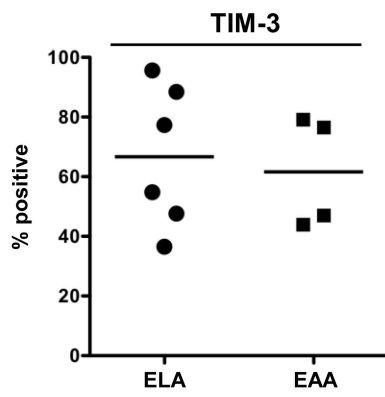


Table S1. Clinical characteristics of patients

Patient	Gender	Age at diagnosis (years)	Disease stage at diagnosis	Type of vaccine ¹	# of vaccines	Duration ² (mo)	Clinical outcome
LAU 205	M	24	pT2aN1M0	ELA+IFA+CpG	20	22.4	†
LAU 321	M	60	pT3aN0M0,IIa	ELA+IFA+CpG	8	7.5	
LAU 371	F	30	pT3aN1M0,III	ELA+IFA+CpG	6	6.1	†
LAU 444	F	28	pT3aN0M0	ELA+IFA+CpG	20	21.9	†
LAU 618	F	70	pT4N0M0	ELA+IFA+CpG	12	11.9	
LAU 672	M	35	pT1N0M0	ELA+IFA+CpG	4	2.8	†
LAU 818	M	55	pT3bN0M0,IIb	ELA+IFA+CpG	18	20.5	
LAU 936	F	52	pT3aN0M0,IIa	ELA+IFA+CpG	7	7.0	†
LAU 944	F	20	pT1aN0M0	ELA+IFA+CpG	16	16.3	
LAU 1164	M	52	pTxNxM1a	ELA+IFA+CpG	14	36.0	
LAU 972	F	60	pT2bN1M0	EAA+IFA+CpG	20	21.5	
LAU 975	M	52	pT4N1bM0	EAA+IFA+CpG	4	2.9	†
LAU 1013	M	56	pT3bN3M0	EAA+IFA+CpG	8	8.4	†
LAU 1015	M	75	pT2aN0M1a,IV	EAA+IFA+CpG	20	22.4	†
LAU 1106	M	36	pT2aN1M0,IIIa	EAA+IFA+CpG	27	44.8	

¹ ELA refers to the analog Melan-A/MART-1 peptide and EAA to the native unmodified peptide

² Time (months) during which the patient received monthly vaccinations

† Death